

Optimization of material removal rate for orthogonal cutting with vibration limits

Márta Janka Reith / Gábor Stépán

Received 2012-06-30

Abstract

Besides growing accuracy requirements for cut parts the maximisation of productivity has still an important role in industry. One possible measure for productivity in cutting processes is the material removal rate. This study deals with the optimisation of the material removal rate considering the bounds set by vibrations through an analytical approach. The damping ratio region was determined, for which the identified local optima with respect to the maximal material removal rate hold.

Keywords

Optimisation · material removal rate · stability · chatter

1 Introduction

An optimal machining strategy always depends on the determined objective function. Efficiency can be measured according to several criteria. These can be: cost effectiveness, minimal/optimal time, optimal usage of capacity, surface quality of the workpiece, tolerances and accuracy, minimal specific energy consumption and lifetime. A further measure can be productivity, which is closely connected to the material removal rate.

Besides well constructed objective functions, there are several conditions an engineer has to deal with when the task is to develop an optimal machining strategy. One group of restricting conditions are the quality requirements for the surface of a machined workpiece and the accuracy. Furthermore, there exist bounds for parameters belonging to each part of the system, the technology, the machine, the tool, the chuck and the workpiece. There are also factors, which cannot be determined from catalogues yet, for example the boundaries of chatter-free (stable) regions of a machining process.

The surface quality of the workpiece is highly effected by vibrations occurring on machine tools. Due to the direct contact between tool and workpiece, the motion of the tool directly shapes the workpiece surface. There is a variety of reasons causing vibrations, which can be handled by means of active or passive vibration elimination methods, but dealing with chatter vibrations is a far more complicated issue. The source of these self-excited vibrations is, on the one hand, the regenerative effect caused by the feedback between subsequent cuts modulating the chip thickness [1, 2]. On the other hand, mode coupling can cause self-excited vibrations during machining, but for the investigations in this study, only the regenerative effect for the chip thickness is taken into consideration, since chatter caused by the mode coupling effect occurs later for most machining cases [3]. The target of the presented study is to present an analytical approach for the maximisation of the material removal rate (MRR) taking into account the bounds set by vibrations.

One of the most important objectives in industry nowadays is maximising productivity, since it is directly connected to machining costs. Productivity can be measured via the MRR. For milling, Budak and Tekeli [4] showed a method for increasing

Márta Janka Reith

Department of Applied Mechanics, BME, H-1111, Budapest, Műegyetem rkp. 5, Hungary
e-mail: reith@mm.bme.hu

Gábor Stépán

Department of Applied Mechanics, BME, H-1111, Budapest, Műegyetem rkp. 5, Hungary
e-mail: stepan@mm.bme.hu

the chatter free MRR. If we increase the material removal rate by increasing the depth of cut, there is a risk of tool breakage. Since chatter vibrations affect the surface quality of the workpiece, the aim is to avoid unstable cutting and restrict machining to the stable parameter region. According to this, the risk of tool breakage does not appear for the investigated conditions, since too high depth of cut values certainly belong to the unstable machining region.

2 Mechanical model and stability diagram for orthogonal turning process

The simplest model for examining the stability loss due to the regenerative effect in cutting mechanisms is the orthogonal turning model. For this special case, the chip thickness h is equal to the feed, the width of cut w is equal to the depth of cut. The orthogonal cutting process can mathematically be described by means of a single degree-of-freedom model (Fig. 1) [5]

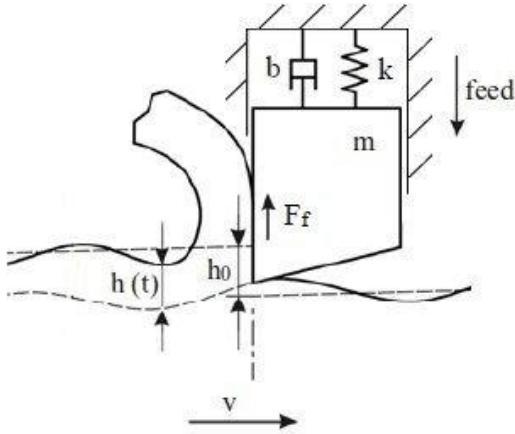


Fig. 1. DoF orthogonal turning model

The feed cutting force can be determined according to the well known “three-quarter rule” [6, 7]:

$$F_y = k_y h^{3/4} w^{1.1} v^{-0.1}. \quad (1)$$

A simplified formula for the feed cutting force is:

$$F_f = k_f h^{3/4} w, \quad (2)$$

where k_y and k_f are cutting constants in feed direction and v is the cutting velocity. The graph of the feed cutting force as a function of the chip thickness can be seen in Fig. 2.

The equation of motion can be expressed as follows (see Fig. 1):

$$m\ddot{y}(t) + b\dot{y}(t) + ky(t) = F_f, \quad (3)$$

where the lumped parameters, by means of which the tool can be modeled are m , the modal mass of the tool, b , the damping coefficient and k , the stiffness. The natural frequency of the tool can be determined by $\omega_n = \sqrt{\frac{k}{m}}$. The regenerative effect should be taken into account, when the chip thickness changes dynamically. The instantaneous value of the chip thickness decreases

by the instantaneous tool displacement, but increases by the displacement of the tool in the previous revolution, which can be expressed as follows (see Fig. 1):

$$h(t) = h_o + y(t - \tau) - y(t), \quad (4)$$

where h_o is the desired or theoretical chip thickness and $[y(t - \tau) - y(t)]$ is the dynamic one. Substituting these relations into the equation of motion, we obtain the simplest form of a mathematical model that includes regenerative chatter for machine tools:

$$m\ddot{y}(t) + b\dot{y}(t) + ky(t) = k_f w (h_o + y(t - \tau) - y(t))^{3/4}. \quad (5)$$

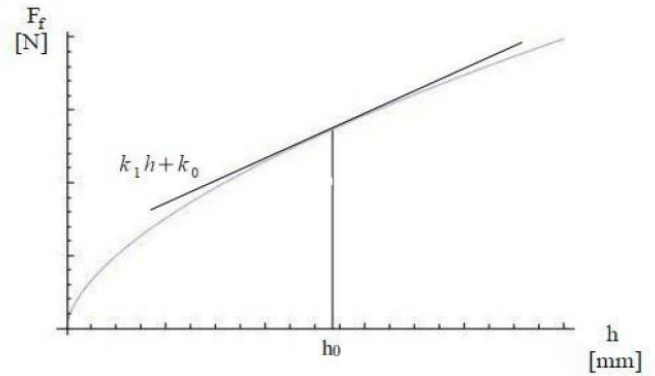


Fig. 2. Typical feed cutting force as a function of chip thickness

The displacement of the tool can be written as the sum of a stationary displacement y_o and an $\eta(t)$ “small” vibration (or perturbation) about the stationary position $y(t) = y_o + \eta(t)$. Furthermore, for the stationary state, the following holds for the feed cutting force:

$$F_f = ky_o = k_f w h_o^{3/4}. \quad (6)$$

If this expression is substituted to the equation of motion, it modifies to the following form:

$$m\ddot{\eta}(t) + b\dot{\eta}(t) + k(y_o + \eta(t)) = k_f w (h_o + \eta(t - \tau) - \eta(t))^{3/4}. \quad (7)$$

After performing a Taylor expansion, and neglecting the higher order terms of the “small” perturbation, one ends up with the following equation of motion:

$$\ddot{\eta}(t) + 2\zeta\omega_n\dot{\eta}(t) + \omega_n^2\eta(t) = \frac{k_1}{m}(\eta(t - \tau) - \eta(t)), \quad (8)$$

where $k_1 = \frac{\partial F}{\partial h}|_{h_o} = \frac{3}{4}k_f w h_o^{-1/4}$ is the cutting coefficient and $\zeta = \frac{b}{2\sqrt{mk}}$ is the damping ratio. The corresponding characteristic equation is:

$$\lambda^2 + 2\zeta\omega_n\lambda + \omega_n^2 + \frac{k_1}{m} - \frac{k_1}{m}e^{-\lambda\tau} = 0, \quad (9)$$

which implies infinitely many characteristic roots. For stability investigations, the stability boundary at $\lambda = i\omega$ has to be checked. With the help of the D-subdivision method, the cutting coefficient can be expressed as:

$$k_1 = \frac{m(\omega^2 - \omega_n^2)^2 + 4\zeta^2\omega_n^2\omega^2}{2(\omega^2 - \omega_n^2)}, \quad (10)$$

from which we obtain the depth of cut at the stability boundary:

$$w = \frac{2}{3} \frac{mh_o^{1/4}}{k_f} \frac{(\omega^2 - \omega_n^2)^2 + 4\zeta^2 \omega_n^2 \omega^2}{(\omega^2 - \omega_n^2)}. \quad (11)$$

Analogously, a formula can be deduced for the spindle speed:

$$\Omega = \frac{\omega\pi}{j\pi - \arctg \frac{\omega^2 - \omega_n^2}{2\zeta\omega_n\omega}}, \quad (12)$$

where j is the number of lobes counted from the right (from above) along the spindle speed parameter. For simplifying the treatment of the parameters, it is advisory to generate their dimensionless form according to the following steps:

$$\tilde{\Omega} = \frac{\Omega}{\omega_n}, \quad (13)$$

$$\tilde{w} = \frac{k_1}{k}, \quad (14)$$

which implies:

$$\tilde{\Omega} = \frac{\tilde{\omega}}{j - \frac{1}{\pi} \arctg \frac{\tilde{\omega}^2 - 1}{2\zeta\tilde{\omega}}}, \quad (15)$$

$$\tilde{w} = \frac{1}{2} \frac{(\tilde{\omega}^2 - 1)^2 + 4\zeta^2 \tilde{\omega}^2}{\tilde{\omega}^2 - 1}, \quad (16)$$

where $\tilde{\omega} = \frac{\omega}{\omega_n}$ is the frequency ratio. For fixed machine tool parameters, the stability diagram can be plotted in the plane of the dimensionless depth of cut and spindle speed. Typical stability digrams can be seen in Fig. 3 for three different damping ratios.

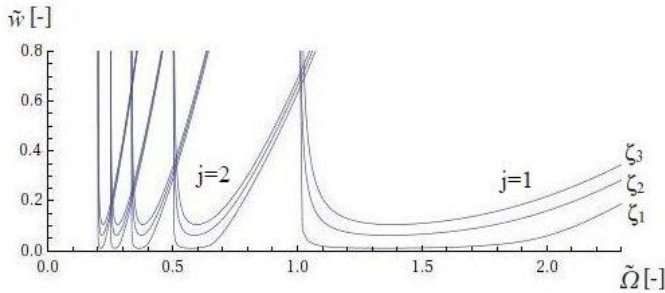


Fig. 3. Stability boundaries for $\zeta_1 = 0.005$, $\zeta_2 = 0.03$, $\zeta_3 = 0.05$

3 Maximising the MRR

Since the optimization of the MRR is a very important aspect for cutting technologies, it necessitates the investigation of machining parameters, which belong to the maximal MRR within the stable machining region.

A curve indicating constant MRR in the plane of the depth of cut and the spindle speed are hyperbolic according to the next formula:

$$w = \frac{2MRR}{h_o d \Omega}. \quad (17)$$

where d is the diameter of the machined workpiece. With the use of dimensionless parameters, we introduce the new parameter k_{MRR} and reformulate the above relation as:

$$\tilde{w} = \frac{k_{MRR}}{\tilde{\Omega}}, \quad (18)$$

where $k_{MRR} = \frac{3}{2} \frac{k_f MRR}{kh_o^{5/4} d \omega_n}$. The stability boundary is the border between the stable and the unstable parameter region, thus we have to analyse the boundary curve. We assume, that there will be local optima for the MRR in the intersection points of two adjacent instability lobes, where the MRR is maximal. Thus, the intersection points of two adjacent lobes have to be calculated, which can be done by setting the equations for two adjacent lobes indexed by j and $j+1$ equal:

$$\frac{1}{2} \frac{(\tilde{\omega}_1^2 - 1)^2 + 4\zeta^2 \tilde{\omega}_1^2}{(\tilde{\omega}_1^2 - 1)} = \frac{1}{2} \frac{(\tilde{\omega}_2^2 - 1)^2 + 4\zeta^2 \tilde{\omega}_2^2}{(\tilde{\omega}_2^2 - 1)}, \quad (19)$$

$$\frac{\tilde{\omega}_1}{j - \frac{1}{\pi} \arctg \frac{\tilde{\omega}_1^2 - 1}{2\zeta\tilde{\omega}_1}} = \frac{\tilde{\omega}_2}{j + 1 - \frac{1}{\pi} \arctg \frac{\tilde{\omega}_2^2 - 1}{2\zeta\tilde{\omega}_2}}. \quad (20)$$

Solving Equation (19) for $\tilde{\omega}_1$, one obtains 4 solutions. Solutions 1 and 2 are $\tilde{\omega}_1 = -\tilde{\omega}_2$, $\tilde{\omega}_1 = \tilde{\omega}_2$, which belong to the case when the two lobes are identical, which naturally is not a usable solution to the problem. Solution 3 is:

$\tilde{\omega}_1 = \frac{-\sqrt{-1+\tilde{\omega}_2^2+4\zeta^2}}{\sqrt{-1+\tilde{\omega}_2^2}}$, which belongs to the lower lobe system for $\omega < \omega_n$. The lower lobe structure refers to negative cutting coefficient values. Since the dimensionless form of the depth of cut was obtained according to Formula Eq. 14, it is directly proportional to the cutting coefficient. The cutting coefficient indeed is negative in some special cases of drilling and milling, for those cases the lower lobe structure is relevant. In the present study, the investigated machining technology is turning, for which the cutting coefficient is positive (see also Fig. 2), thus, the region belonging to negative cutting coefficients is of no interest. Thus, the solution related to the specified parameter region is Solution 4:

$\tilde{\omega}_1 = \frac{\sqrt{-1+\tilde{\omega}_2^2+4\zeta^2}}{\sqrt{-1+\tilde{\omega}_2^2}}$. This can be substituted back into Equation (20), which implies an implicit equation including trigonometric functions that has no closed-form solution, thus can only be solved numerically.

$$\frac{-\tilde{\omega}_2}{(j+1)\pi + \arctan \frac{1-\tilde{\omega}_2^2}{2\tilde{\omega}_2\zeta}} + \frac{L_1}{j\pi - \arctan \frac{2\zeta}{(\tilde{\omega}_2^2-1)L_1}} = 0 \quad (21)$$

where $L_1 = \sqrt{1 + \frac{4\zeta^2}{\tilde{\omega}_2^2 - 1}}$.

The ζ damping ratio parameters, for which the stability lobes were plotted in Fig. 4 are not taken from the realistic physical range of damping ratios for machine tools, which normally is in the range of $\zeta = 0.01 \div 0.03$. Still carrying out the calculations for those high damping ratios was necessary for mathematical investigations explained later.

Assuming certain values for ζ and j , $\tilde{\omega}_2$ values can be calculated accordingly. By means of the solutions for $\tilde{\omega}_1$ and $\tilde{\omega}_2$, one is able to calculate the intersection points of two adjacent lobes on the $\tilde{\Omega} - \tilde{w}$ plane. Results for intersection point coordinates can be found in the Appendix for the following ζ values: 0.001, 0.003, 0.005, 0.01, 0.03, 0.05, 0.1, 0.3, 0.5. Since the values of \tilde{w} and $\tilde{\Omega}$ in the intersection points are known, the constants of

Tab. 1. Result for kMRR for the hyperbolas crossing the first five intersection points of two adjacent lobes

	$\zeta = 0.001$	$\zeta = 0.003$	$\zeta = 0.005$	$\zeta = 0.01$	$\zeta = 0.03$	$\zeta = 0.05$	$\zeta = 0.1$	$\zeta = 0.3$	$\zeta = 0.5$
1	0,62761	0,63286	0,63814	0,65145	0,70644	0,76425	0,92137	1,73845	2,87889
2	0,14159	0,14354	0,14550	0,15047	0,17138	0,19394	0,25759	0,61760	1,15423
3	0,06076	0,06191	0,06307	0,06603	0,07867	0,09256	0,13266	0,36764	0,72482
4	0,03360	0,03441	0,03523	0,03733	0,04639	0,05650	0,08609	0,26218	0,53156
5	0,02131	0,02193	0,02256	0,02419	0,03128	0,03927	0,06290	0,20435	0,42112

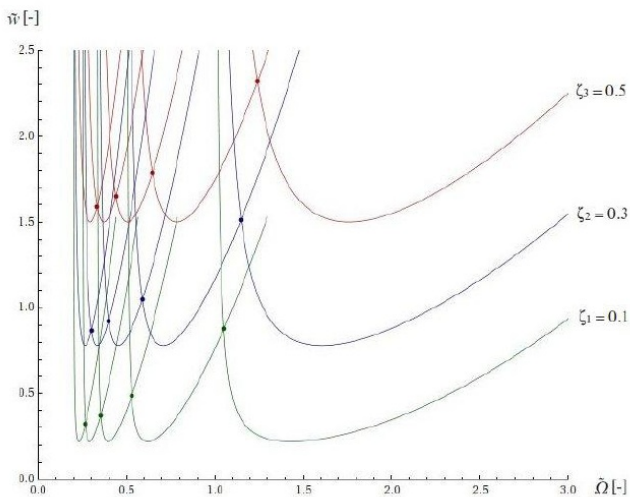


Fig. 4. Stability diagram and intersection points of two adjacent lobes for ζ values: 0.1, 0.3, 0.5.

the hyperbolas crossing the intersection points can be calculated according to:

$$k_{MRR} = \tilde{w}\tilde{\Omega}. \quad (22)$$

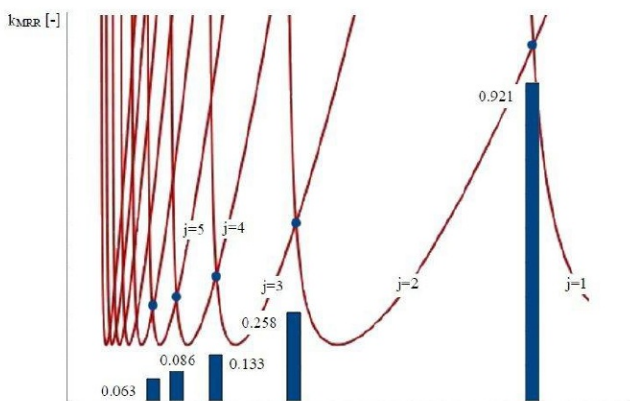


Fig. 5. Tendency of k_{MRR} values for the hyperbolas crossing the first five intersection points of two adjacent lobes ($\zeta = 0.1$)

The numerically calculated values of the dimensionless constants k_{MRR} of the hyperbolas are presented in Tab. 1.

As it is visible from the numerical results and Fig. 5, the dimensionless constant k_{MRR} is larger at the intersection points of the lobes belonging to smaller j values.

For the lower $\tilde{\Omega}$ region, for example at machining point H , it is more favourable for higher MRR to move to point G , since the increase of the spindle speed is not significant, but much higher MRRs can be realized. Furthermore, if we examine points E and F , the MRR can naturally be increased by applying higher depth of cut values.

For turning processes, the trends of the last decades show an increase of the applied cutting speeds. One reason for shifting technological parameters towards high spindle speeds is the growing accuracy requirements. W continuously grows, which results smaller deformations on the workpiece. This can be realized by means of shifting the number of revolutions to higher regions, which implies smaller cutting forces (see Formula 1). The super-hard tool materials used today, like CBN or pCBN are able to resist high velocities, but because of their rigidity they are not able to withstand high chip load. The tools made out of these materials have their optimal lifetime when they are applied for high speed machining. Furthermore, this is the reason for avoiding high depths of cuts for these tools.

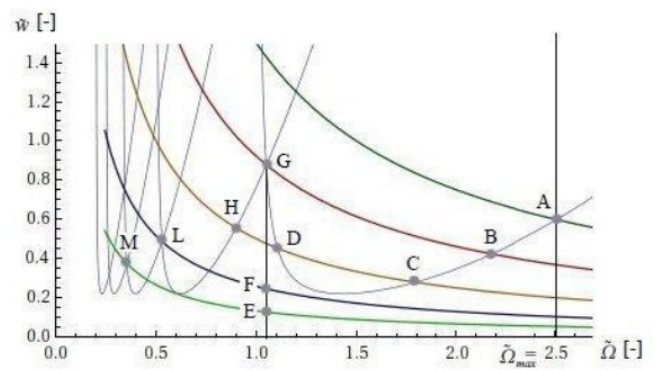


Fig. 6. Stability diagram with constant MRR curves and characteristic points for ($\zeta = 0.1$)

In order to find the points, where the maximal MRR can be achieved locally, we refer back to Fig. 6. The analysed interval for the spindle speed is marked by vertical lines. If we accept the stability diagram computed for given parameters, it can be deduced, that the maximal available MRR for the examined interval of the spindle speed is at point A . However, if we cannot exploit the maximal spindle speed of the machine tool and we can only go up to $\tilde{\Omega}_B$, then the maximal available material removal rate is the one belonging to the hyperbola crossing the

lobe at point B . The MRR is the same for point G and B , thus it is necessary to find further criteria to be able to judge, which point is more favourable. As mentioned in the introduction, this depends on the objective functions, whether surface quality or minimal energy consumption has to be achieved.

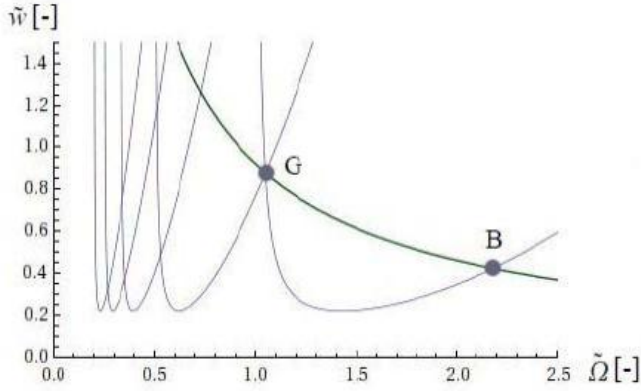


Fig. 7. Judging points B and G

The next criteria for judging the two machining points B and G in this work is the specific energy required for chip removal.

The points are on the same hyperbola representing one specific material removal rate, thus $MRR_B = MRR_G$ holds. Lets

assume, that the feed is set to the same value in both cases and the cutting constant k_f between the two points stays constant. Furthermore, the machined radius for the two cases is assumed to be the same, too. The specific energy required for removing unit chip volume is:

$$E_V = \frac{E}{V}, \quad (23)$$

where V is the chip volume $V = wh_0s$ and the required energy is $E = F_y s$, where s is the length of the cut path.

The following relation holds between the depth of cut and the spindle speed:

$$w = \frac{c}{\Omega}, \quad (24)$$

where $c = \frac{2MRR}{h_0 d}$. Substituting Formula Eq. 1 and Eq. 24 into Eq. 23 one ends up with the following expression:

$$E_V = \frac{2^{0.1} k_y h^{-1/4} c^{0.1}}{d^{0.1}} \frac{1}{\Omega^{0.2}}. \quad (25)$$

From this result we can draw the conclusion, that the specific energy required for chip removal is smaller at the point, where the spindle speed is larger, thus the energy required for removing a unit chip volume at point B is less compared to point G .

A further aspect that can be included in judging the machining points is to avoid resonance. For milling operations the stability diagram is obtained by means of a more complex calculation due to parametric excitation, but the described considerations for local optima can be used well. The amplitude of the vibration resulting from the forced excitation occurring for milling operations will be larger at point G at the left asymptote of the lobes. Thus also from this point of view point B is more favourable.

4 Are the intersection points of two adjacent lobes always local optima referring to maximal MRR?

As previously mentioned, the requirement for stable cutting holds. Since the aim is to find the machining point, where the MRR is maximal, it is advisory to have a look at the intersection point of the lobes first, which are situated on the boundary of the stability region. If the tangent of the right lobe involved in the intersection is steeper at the intersection point than the tangent of the hyperbola crossing the afore mentioned point, it implies that there is a local optimum with respect to the maximal MRR in that point. If this holds, small increase of the spindle speed does lead to lower MRRs. In order to prove, that the local optimum point always can be found in the intersection point of two adjacent lobes it is necessary to show that the derivative of the right lobes in the intersection points t_L is always bigger in absolute value than the derivative of the hyperbolas crossing the intersection points t_H , since both are negative. The derivative of a parametrically defined function can be computed according to the following relation:

$$\frac{d\tilde{w}}{d\tilde{\Omega}} = \frac{d\tilde{w}}{d\tilde{\omega}} / \frac{d\tilde{\Omega}}{d\tilde{\omega}}, \quad (26)$$

which results:
$$\frac{d\tilde{w}}{d\tilde{\Omega}} = \frac{1 + \frac{4\zeta^2}{\omega_1^2 - 1} - \frac{\omega_1^2}{\omega_1^2 - 1}}{\frac{1}{2D} \left(1 + \frac{1}{\omega_1^2} \right) + \frac{1}{\omega_1 L_2}}}, \text{ where } L_2 = j - \frac{\arctan \frac{\omega_1^2 - 1}{2\omega_1 \zeta}}{\pi}.$$

The derivative of the hyperbolas has the following form:

$$\frac{d\tilde{w}}{d\tilde{\Omega}} = \frac{-k_{MRR}}{\tilde{\Omega}^2}.$$

One possible way of comparing the value of the two derivatives can be done by taking their ratio:

$$\tilde{t} = \frac{t_L}{t_H}. \quad (27)$$

Tab. 2: Values of \tilde{t} for the first five lobes for given ζ values

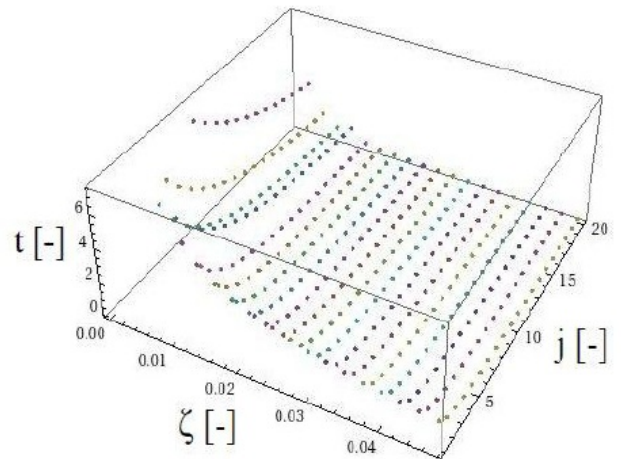


Fig. 8. Distribution of \hat{t} as a function of the parameters j and ζ

Tab. 2. Values of \tilde{t} for the first five lobes for given ζ values

	$\zeta = 0.001$	$\zeta = 0.003$	$\zeta = 0.005$	$\zeta = 0.01$	$\zeta = 0.03$	$\zeta = 0.05$	$\zeta = 0.1$	$\zeta = 0.3$	$\zeta = 0.5$
1	1963,5200	654,5120	392,7010	184,0350	54,2178	28,9596	19,2903	6,0323	3,4364
2	1766,1300	587,9810	352,3140	157,4570	42,4071	20,9299	15,6276	4,1114	2,1579
j 3	1699,6800	565,0980	338,0990	144,4020	35,7763	16,3767	13,3790	3,0928	1,5616
4	1665,9500	553,1010	330,3860	135,0320	30,8665	13,0546	11,6537	2,4600	1,2183
5	1645,3100	545,4380	325,2430	127,3480	26,8790	10,3995	10,2676	2,0333	0,9967

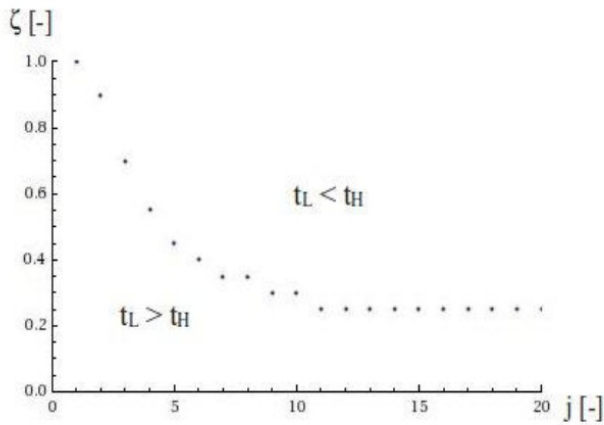


Fig. 9. Representation of the regions $t_L > t_H$ and $t_L < t_H$

Tab. 2 shows the values of \tilde{t} for the first five lobes and certain damping ratios. If the ratio number is greater than one: $\tilde{t} > 1$, than the intersection point is a local optimum point for the MRR. If $\tilde{t} < 1$, than the hyperbola is steeper and the continuous increase of the spindle speed would imply higher and higher MRRs along the lobes.

The t values as a function of the parameters j and ζ are shown in Fig. 8. The smaller the

damping ratio and the smaller the number of lobes, the higher values for the ratio of derivatives we obtain. It is visible, that for higher lobe numbers and stronger damping the ratio even gets smaller than one, which necessitates to examine, for which parameter region the statement about the local optimum holds. This was done numerically in discrete points of j and ζ .

The evolution of the boundary between the two regions reminds on an exponential function, which is presented in Fig. 9. Results show, that at least up to the value of $\zeta = 0.25$ even in small spindle speed regions the local optimum for the MRR will be in the intersection point of two adjacent lobes.

Furthermore the observation was made, that in the high spindle speed region the statement for the local optimum of the MRR even holds for very high damping ratios. This is an important finding, since there are CNC machines with high damping ratios, for which these investigations can be of high importance.

5 Conclusion

In the model considered in this study an optimization was done with respect to the maximal material removal rate along a theoretical approach. The damping ratio region was determined, for which the local optimum of the MRR are situated in the intersection points of two adjacent lobes on the stability diagram. For the conventional damping ratio region for CNC machines the statement about the local optima referring to maximal MRR always holds. It was found, that in the high spindle speed region the local optimum for the MRR even holds for very high damping ratios, which is important for special highly damped CNC machine tools. For the applied model for orthogonal cutting the regenerative effects are taken into account. Besides this regenerative effect there are much more parameters influencing the stability properties of the cutting process, such as the eccentricity of the spindle, the ovality of the workpiece, eventually material inhomogenities and many more, which were not taken into consideration in this study. It is a further goal to determine the effect of the mentioned possible effects on the stability of the turning process, because it is possible, that they have more significant influence on the vibration amplitudes for machining processes.

References

- 1 **Tobias SA**, *Machine Tool Vibration*, Blackie and Sons Ltd., 1969.
- 2 **Tlustý J, Poláček M**, *The Stability of Machine Tools against Self Excited Vibrations*, ASME Int. Research in Production Eng. (1963), 465–474.
- 3 **Altintas Y**, *Manufacturing Automation*, Cambridge University Press, 2000.
- 4 **Budak E, Tekeli A**, *Maximizing Chatter Free Material Removal Rate in Milling through Optimal Selection of Axial and Radial Depth of Cut Pairs*, CIRP Annals – Manufacturing Technology **54** (2005), 353–356, DOI 10.1016/S0007-8506(07)60121-8.
- 5 **Stépán G**, *Retarded mechanical systems: stability and characteristics functions*, Longman Scientific & Technical, New York, 1989.
- 6 **Taylor WF**, *On the art of cutting metals*, Trans Am. Soc. Eng **28** (1907), 31–350.
- 7 **Kienzle O**, *Spezifische Schnittkräfte bei der Metallbearbeitung*, Werkstattstechnik und Maschinenbau **47**, 224–225.

Tab. 3. Coordinates of intersection points for two adjacent lobes for given ζ parameters

$\zeta = 0.001$					$\zeta = 0.01$				
	ω_1	ω_2	$\tilde{\Omega}$	\tilde{w}		ω_1	ω_2	$\tilde{\Omega}$	\tilde{w}
1	1,00000	1,50153	1,00051	0,62729	1	1,00015	1,51512	1,00509	0,64815
2	1,00000	1,25141	0,50028	0,28302	2	1,00033	1,26388	0,50285	0,29923
j 3	1,00001	1,16803	0,33353	0,18216	j 3	1,00051	1,18001	0,33531	0,19692
4	1,00001	1,12634	0,25015	0,13433	4	1,00068	1,13802	0,25152	0,14842
5	1,00001	1,10133	0,20012	0,10647	5	1,00084	1,11278	0,20124	0,12018

$\zeta = 0.003$					$\zeta = 0.03$				
	ω_1	ω_2	$\tilde{\Omega}$	\tilde{w}		ω_1	ω_2	$\tilde{\Omega}$	\tilde{w}
1	1,00001	1,50457	1,00153	0,63190	1	1,00130	1,54448	1,01527	0,69582
2	1,00003	1,25422	0,50085	0,28658	2	1,00270	1,29031	0,50862	0,33696
j 3	1,00005	1,17074	0,33392	0,18539	j 3	1,00397	1,20500	0,33939	0,23180
4	1,00007	1,12900	0,25045	0,13740	4	1,00512	1,16208	0,25470	0,18215
5	1,00008	1,10395	0,20037	0,10945	5	1,00617	1,13616	0,20386	0,15342

$\zeta = 0.005$					$\zeta = 0.05$				
	ω_1	ω_2	$\tilde{\Omega}$	\tilde{w}		ω_1	ω_2	$\tilde{\Omega}$	\tilde{w}
1	1,00004	1,50760	1,00255	0,63652	1	1,00339	1,57284	1,02543	0,74531
2	1,00009	1,25700	0,50142	0,29017	2	1,00682	1,31539	0,51448	0,37697
j 3	1,00013	1,17343	0,33432	0,18865	j 3	1,00977	1,22847	0,34359	0,26940
4	1,00018	1,13162	0,25076	0,14051	4	1,01233	1,18454	0,25802	0,21897
5	1,00022	1,10652	0,20061	0,11247	5	1,01457	1,15793	0,20662	0,19007

$\zeta = 0.1$				
	ω_1	ω_2	$\tilde{\Omega}$	\tilde{w}
1	1,00012	1,64017	1,05070	0,87691
2	1,00023	1,37408	0,52941	0,48657
j 3	1,00031	1,28322	0,35445	0,37425
4	1,00038	1,23703	0,26666	0,32284
5	1,00043	1,20900	0,21385	0,29416

$\zeta = 0.3$				
	ω_1	ω_2	$\tilde{\Omega}$	\tilde{w}
1	1,00071	1,87705	1,14901	1,51300
2	1,00120	1,57952	0,58940	1,04785
j 3	1,00152	1,47647	0,39851	0,92253
4	1,00175	1,42409	0,30167	0,86911
5	1,00192	1,39241	0,24294	0,84113

$\zeta = 0.5$				
	ω_1	ω_2	$\tilde{\Omega}$	\tilde{w}
1	1,00150	2,08279	1,24155	2,31879
2	1,00238	1,75923	0,64622	1,78613
j 3	1,00292	1,64669	0,43984	1,64792
4	1,00327	1,58942	0,33416	1,59073
5	1,00352	1,55475	0,26970	1,56142